

INFLUENCE OF ICE CONDITIONS  
ON THE EFFECTIVENESS OF THE RESONANT  
METHOD OF BREAKING ICE COVER BY SUBMARINES

V. M. Kozin,<sup>1</sup> S. D. Chizhumov,<sup>2</sup> and V. L. Zemlyak<sup>2</sup>

UDC 532.59:629.585:534.1

*This paper describes a numerical model for analyzing the stress–strain state of ice cover which has fractures of various widths caused by hydrodynamic loads due to submarine motion. Calculations and experiments were performed using the model of unbreakable ice, and the results were used to obtain dependences of the amplitude of deflections and stress in ice cover on the width of the ice fracture. The behavior of ice cover under wave loading was studied.*

**Key words:** flexural-gravity waves, resonant method of breaking ice, resonant velocity, submarine, ice conditions.

1. At present, wide experience has been gained with the operation of nuclear submarines making long passages under ice in the North. However, emergency situations can arise when a submarine needs to surface through continuous ice cover. As a rule, surfacing of a submarine vessel (SV) is accomplished by producing a static load on ice from below due to creation of positive buoyancy by draining the ballast tanks. This method of surfacing, however, has a number of drawbacks (insignificant thickness of broken ice, necessity of increasing the structural limit, possibility of instability etc.). These drawbacks can be eliminated by subjected ice cover to hydrodynamic loads which arise near the bottom surface of a moving SV. This possibility has been proved previously by modeling experiments [1–3].

Motion of a SV under ice cover gives rise to flexural-gravity waves, whose amplitude reaches a maximum when the SV velocity exceeds the so-called crest velocity corresponding to the most intense wave formation during motion in ice-free water. It has been shown [1] that the limiting thickness of continuous ice that can be broken by resonant flexural-gravity waves during SV motion is several times greater than that in static breaking of ice cover during surfacing.

The influence of the thickness of continuous ice cover on its stress–strain state and the possibility of its breaking by a SV was studied in [1, 3, 4]. However, complete breaking of ice may require several passages of the vessel: during the first passage, one or several cracks are formed, and subsequent passages lead to further ice breaking. The present paper deals with the influence of an open longitudinal crack or ice fracture of various widths on the deflections and stresses arising in ice cover during SV motion.

2. The equation of deformations of a viscoelastic homogeneous plate (ice cover) under dynamic loading is written as

$$D\nabla^4 w + D\tau\nabla^4 \dot{w} + \beta\dot{w} + \rho_s h\ddot{w} = p, \quad (1)$$

where  $w$ ,  $\dot{w}$ , and  $\ddot{w}$  are functions of the deflection, normal velocity, and normal acceleration of the plate which depend on the coordinates of the plate surface  $x$  and  $y$  and time  $t$ ,  $D = Eh^3/(12(1 - \nu^2))$  is the cylindrical rigidity,  $E$  is the elastic modulus,  $\nu$  is Poisson's ratio,  $\rho_s$  is the density of the plate material,  $\tau$  is the stress relaxation time,

---

<sup>1</sup>Komsomol'sk-on-Amur State Technical University, Komsomol'sk-on-Amur 681013. <sup>2</sup>Institute of Machine Science and Metallurgy, Far East of the Russian Academy of Sciences, Komsomol'sk-on-Amur 681005; velkom@list.ru. Translated from *Prikladnaya Mekhanika i Tekhnicheskaya Fizika*, Vol. 51, No. 3, pp. 118–125, May–June, 2010. Original article submitted January 12, 2009; revision submitted June 10, 2009.

$\beta$  is the viscous drag coefficient,  $h$  is the thickness of the plate, and  $h$  is the pressure field which arises during SV motion.

Because, during bending of ice cover, the displacements, velocities, and accelerations are small in comparison with the corresponding dimensions of the submarine and parameters of its motion, we use a linear formulation of the hydroelastic problem. The liquid is considered ideal and incompressible. The boundary conditions on the plate are extended to its undeformed surface, and the hydrodynamic loading is given by the formula

$$p = p_0 + p_{st} + p_w, \quad (2)$$

where  $p_0$  is the pressure on the ice surface as a solid wall during SV motion,  $p_{st} = -\rho_w g w$  is the hydrostatic reaction of the liquid to the plate bending,  $\rho_w$  is the density of the liquid, and  $g$  is the gravitational constant. Under the assumption of smallness of the deformation velocities, the liquid inertia force due to plate bending can be determined from the linearized Cauchy–Lagrange integral

$$p_w = -\rho_w \frac{\partial \varphi}{\partial t}, \quad (3)$$

where  $\varphi$  is the liquid velocity potential.

Generally, the floating plate interacts with the waves formed on the water free surface in the ice fracture and behind the outer edges. The case has been considered where the outer edges are at a great distance from the wave source (vessel), and, hence the deformations and the wave effect on the free surface behind the outer edges are insignificant. At the same time, during SV motion in an ice fracture, a wave can form which influences the plate bending by impinging on the edges of the ice plate. In many papers, mathematical modeling of ice bending is performed using a linear condition on the free surface. For example, in [5] a numerical model is given for the case of a load moving along the edge of ice. However, the possibility of using the linear condition needs to be studied as a function of ice fracture width, ice thickness, and the nature of the hydrodynamic load produced by SV motion. Thus, direct numerical and physical modeling of the impact of waves on the free surface in an ice fracture requires additional studies.

The presence of an ice fracture in the ice plate will be considered approximately by assuming that the free surface is covered by a region of the plate whose elastic modulus is two orders of magnitude smaller than the elastic modulus of the plate. This allows us to avoid imposing an additional boundary condition on the free surface and considerably simplifies the modeling.

To determine the hydrodynamic pressure  $p_0$ , we consider SV motion with a specified velocity  $v(t)$ . The liquid velocity field at each time is determined by the solving the boundary-value problem for the Laplace equation:

$$\Delta \varphi(x, y, z) = 0 \quad \text{in } \Omega; \quad (4)$$

$$\frac{\partial \varphi}{\partial n} = v \cos(x, n) \quad \text{on } \Gamma_s; \quad (5)$$

$$\frac{\partial \varphi}{\partial n} = 0 \quad \text{on } \Gamma_w; \quad (6)$$

$$\lim_{R \rightarrow \infty} \varphi = 0, \quad \lim_{R \rightarrow \infty} \frac{\partial \varphi}{\partial n} = 0 \quad \text{on } \Gamma_\infty. \quad (7)$$

Here  $\Omega$  is the region occupied by the liquid,  $\Gamma = \Gamma_s + \Gamma_w + \Gamma_\infty$  is the boundary of the region  $\Omega$ ,  $\Gamma_s$  is the surface SV,  $\Gamma_w$  is the surface of the ice plate,  $\Gamma_\infty$  is the conventional boundary (part of the sphere of radius  $R$  at infinite distance from the vessel),  $n$  is the normal to the liquid boundary, and  $v$  is the forward velocity of the SV.

To determine the hydrodynamic pressure  $p_w$ , we consider elastic deformations of the ice plate at velocity  $\dot{w}$ . The liquid velocity field during each time is determined by solving the boundary-value problem for the Laplace equation (4), (5), (7) with the boundary condition on the ice surface

$$\frac{\partial \varphi}{\partial n} = \frac{\partial w}{\partial t} \quad \text{on } \Gamma_w. \quad (8)$$

These equations are solved simultaneously with the equations of motion of the elastic plate (1), (2). Thus, system (1)–(8) represents a formulation of the hydroelastic problem.

In the case of a continuous ice field (a plate of great extent) in the absence of substantial flows, wave damping and viscous friction of water can be neglected. Then, in view of (2) and (3), the motion of the elastic plate (1) can be described by the equation

$$D\nabla^4 w + D\tau\nabla^4 \dot{w} + \rho_s h \ddot{w} + \rho_w g w + \rho \frac{\partial \varphi}{\partial t} = p_0. \quad (9)$$

The numerical solution of Eq. (9) is constructed using the finite-element method. The ice plate is modeled by isoparametric quadrangular finite elements with a linear approximation of the nodal parameters: deflections and rotation angles. The matrix equation corresponding to Eq. (9) has the form

$$[K]\{q\} + [C]\{\dot{q}\} + [M]\{\ddot{q}\} = \{F_0\}, \quad (10)$$

where  $[K] = [K^*] + [K^w]$  is the rigidity matrix which includes the rigidity matrices for the plate and the elastic base (taking into account hydrostatic forces),  $[C] = \tau$ ,  $[K^*]$  is the matrix of the internal drag coefficients,  $[M] = [M^0] + [\mu]$  is the mass matrix which includes the matrices of inertia of the elastic plate and the adjacent liquid,  $\{q\}$  is the vector of generalized displacements,  $\{F_0\}$  is the vector of the hydrodynamic inertial forces acting on the ice surface during SV motion.

The hydrodynamic effect was determined using the boundary-element method [6]. The boundary between the liquid and the plate was modeled by quadrangular boundary elements with a linear approximation of the velocity potential and its normal derivative, which, according to condition (8), is the normal velocity of motion of the boundary. In this case, the boundary-value problems (4)–(8) are transformed to boundary integral equations, whose finite-element analog can be written as [6]

$$[H]\{\varphi\} = [G]\{v\},$$

where  $[H]$  and  $[G]$  are the coefficient matrices,  $\{\varphi\}$ ,  $\{v\}$  are the vectors of the nodal values of the functions  $\varphi$  and  $\partial\varphi/\partial n$ . Taking into account that the boundary surface consists of two parts ( $\Gamma = \Gamma_s + \Gamma_w$ ), we split the last equation into blocks:

$$\begin{aligned} [H_{ss}]\{\varphi_s\} + [H_{sw}]\{\varphi_w\} &= [G_{ss}]\{v_s\} + [G_{sw}]\{v_w\}, \\ [H_{ws}]\{\varphi_s\} + [H_{ww}]\{\varphi_w\} &= [G_{ws}]\{v_s\} + [G_{ww}]\{v_w\}. \end{aligned} \quad (11)$$

Eliminating the unknowns on the surface of the vessel  $\{\varphi_s\}$  from (11) we obtain

$$\{\varphi_w\} = [H_{ww}^*]^{-1}([G_{ww}^*]\{\dot{w}\} + \{V\}), \quad (12)$$

where

$$\begin{aligned} [H_{ww}^*] &= [H_{ww}] - [H_{ws}][H_{ss}]^{-1}[H_{sw}], & [G_{ww}^*] &= [G_{ww}] - [H_{ws}][H_{ss}]^{-1}[G_{sw}], \\ \{V\} &= ([G_{ws}] - [H_{ws}][H_{ss}]^{-1}[G_{ss}])\{v_s\}. \end{aligned}$$

The normal forces at the nodes exerted on the ice plate by the liquid are expressed in terms of the pressure at the nodes using the distribution vector  $\{N\}$ :

$$\{F_{w0}\} = \{N\}\{p\}.$$

In view of (3) and (12), the hydrodynamic forces at the nodes of the plate are given by the expression

$$\{F_{w0}\} = \{F_w\} + \{F_0\},$$

where

$$\{F_0\} = -\rho_w \frac{\partial}{\partial t} ([N][H_{ww}^*]^{-1}\{V\}), \quad \{F_w^n\} = -\rho_w [N][H_{ww}^*]^{-1}[G_{ww}^*]\{\ddot{w}\} = -[\mu]\{\ddot{w}\}.$$

The algorithm of numerical integration of Eq. (10) over time uses a finite-difference scheme [7] based on a linear approximation of accelerations in a time step.

For this numerical model, software was developed and used [4] to calculate deflections and stresses for a homogeneous plate and to study the effect exerted on them by plate thickness and the velocity of the vessel.

**3.** In the present work, we studied the effect of the width of the ice fracture above the vessel trajectory on the deflections and stresses of an ice plate 0,5 m thick at a relative submergence of the vessel  $h_0/L = 0.2$  ( $h_0$  is the

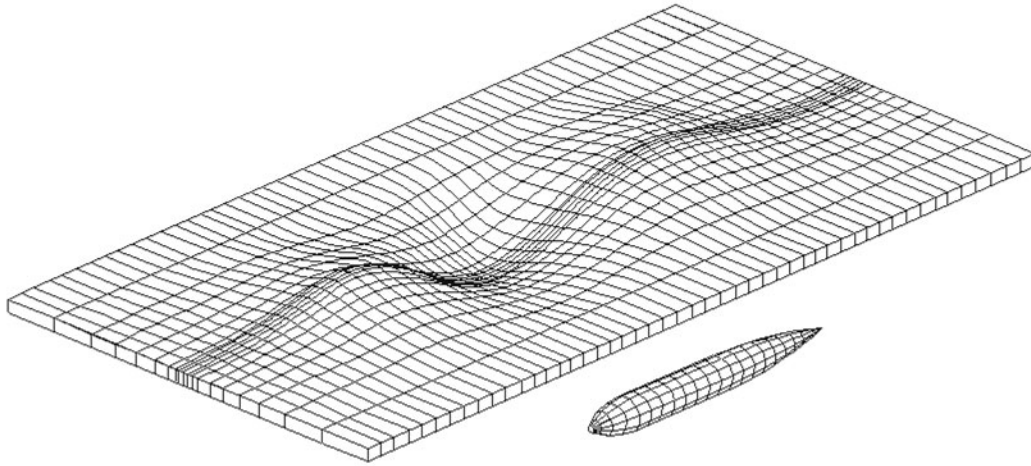


Fig. 1. Computation model of SV motion.

submergence depth reckoned from the longitudinal axis of symmetry of the hull). The SV is represented as a body of revolution (Fig. 1) with a negative length-to breadth ratio  $L/B = 8$  and a draught  $D_n = 12,000$  tons.

It was assumed that the sizes of the finite-element mesh on the surface of the ice plate and the sizes of the boundary-element mesh were identical. In addition, the symmetry of the model about the longitudinal vertical plane was taken into account. The computation step and the parameters of the meshes were chosen from an analysis of the convergence of the calculation results.

The step in time was chosen in the range of 0.2–0.4 sec, depending on the specified velocity of the vessel. The surfaces of the vessel and ice field were partitioned by an irregular mesh (see Fig. 1). The surface of half of the vessel included 280 nodes (21 cross section each containing 15 nodes). The sizes of the computation mesh of the ice plate were chosen on the basis of test calculations so that, at the edges of the plate, the displacements and stresses are much smaller than the maximum values. For example, for an ice thickness of 0.5 m, the length and half-width of the computation mesh were 500 and 100 m, respectively. The mesh contained 500 nodes (50 cross-section sections each containing 10 nodes). The edges of the plate were free.

The values of the resonant velocity of the SV providing the greatest efficiency of dynamic action on the ice cover were determined from the maximum dynamic deflections and stresses of the ice plate. Figures 2 and 3 gives curves of the maximum deflections and stresses on the SV velocity. It is evident that the presence of a longitudinal crack or ice fracture has little effect on the resonant velocity.

The greatest stresses in the ice plate arose at a lower velocity compared to the velocity at which the greatest deflections took place. As a result, the resonant peaks correspond to a certain range of velocities. The calculations show that the resonant velocity increases with increasing ice thickness (Fig. 4).

It should be noted that the most effective destruction of ice cover occurs in the case of SV motion at the resonant velocity under a longitudinal open crack (see Fig. 3). In this case, the maximum longitudinal stress arises in ice, leading to formation of main cracks perpendicular to the direction of motion of the load.

4. To confirm the theoretical results, we studied the behavior of ice cover under wave loading using the model of unbreakable ice.

According to the well-known technique of modeling of flexural-gravity waves in unbreakable continuous ice, the following similarity conditions [8] should be satisfied:

$$\lambda_E = \lambda_w = \lambda_\sigma = \lambda_h = \lambda_l, \quad \lambda_P = \lambda_l^3.$$

Here  $\lambda_l$  is the geometrical scale,  $\lambda_E$  is the model scale for the elastic modulus,  $\lambda_w$  is the model scale for deflections,  $\lambda_\sigma$  is the model scale for stresses,  $\lambda_h$  is the model scale for ice thickness, and  $\lambda_P$  is the model scale for mass forces.

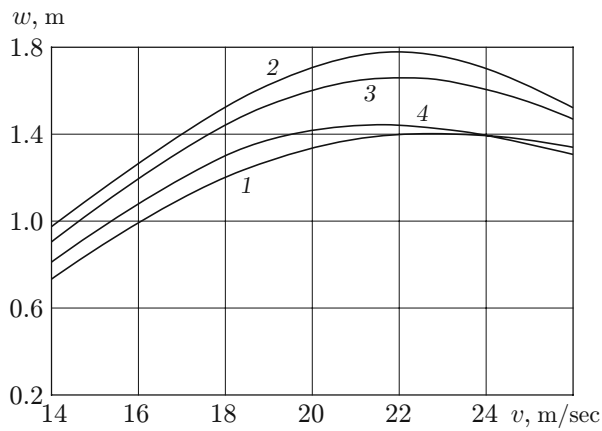


Fig. 2

Fig. 2. Maximum deflections versus SV velocity: 1) continuous ice; 2) longitudinal crack; 3) ice fracture 6 m wide; 4) ice fracture 12 m wide.

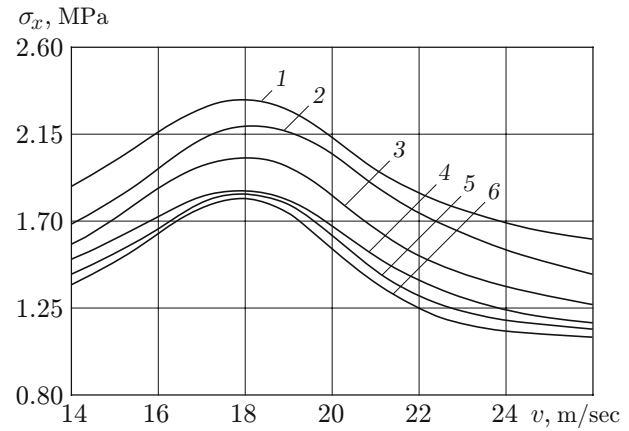


Fig. 3

Fig. 3. Maximum stresses versus SV velocity: 1) longitudinal crack; 2) continuous ice; 3) ice fracture 3 m wide; 4) ice fracture 6 m wide; 5) ice fracture 9 m wide; 6) ice fracture 12 m wide.

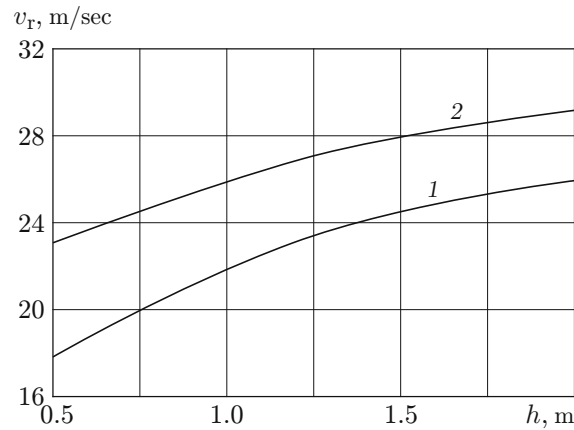


Fig. 4. Resonant velocity versus ice thickness for deflections (1) and stresses (2).

The similarity conditions for Poisson's ratio  $\mu$  and density  $\rho_1$  of ice are not satisfied since they have an insignificant influence on modeling results. If the Froude and Cauchy criteria are satisfied, the velocity of motion of the model  $v_m$  is determined from the condition

$$v_n/v_m = \lambda_l^{1/2}.$$

The parameters of the model flexural-gravity waves are converted to natural waves according to the relations

$$\lambda_n/\lambda_m = A_n/A_m = \lambda_l, \quad T_n/T_m = \lambda_l^{1/2},$$

where  $\lambda_n$  is the length of natural waves,  $\lambda_m$  is the length of the model waves,  $A_n$  is the amplitude of natural waves,  $A_m$  is the amplitude of the model waves,  $T_n$  is the period of natural waves, and  $T_m$  is the period of the model waves.

As the model of ice we used sheet rubber as the most accessible material. The value of the elastic modulus of rubber was determined in tension experiments at various loading rates on a special bench. The average value of the elastic modulus was  $E_m = 2.5$  MPa, which made it possible to perform studies on a scale  $\lambda_l = 500$ , i.e., for modeling ice 0.5 m thick, we used rubber 1 mm thick.

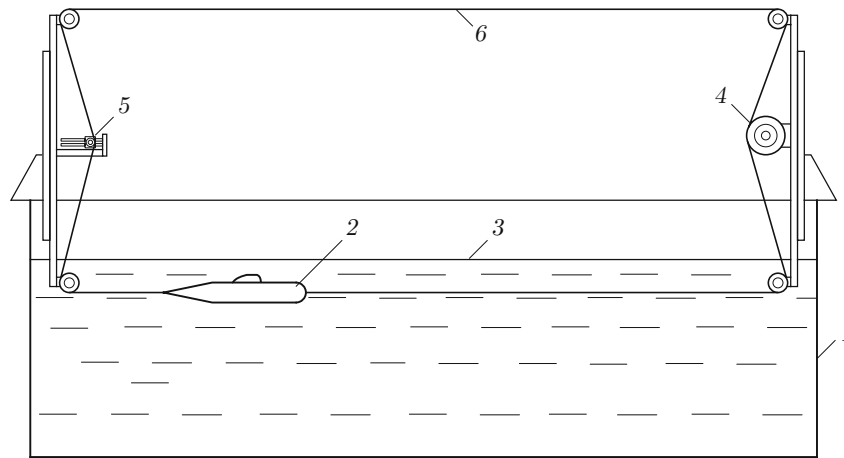


Fig. 5. Diagram of experimental setup: 1) tank; 2) submarine model; 3) continuous ice model; 4) drive; 5) guide pulley; 6) infinite towing cable.

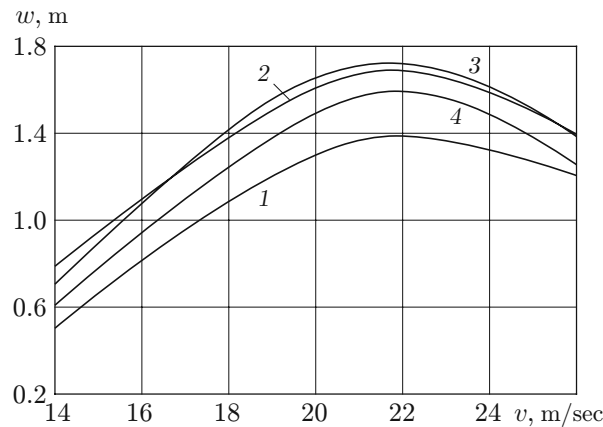


Fig. 6. Maximum deflections versus SV velocity: 1) continuous ice; 2) longitudinal crack; 3) ice fracture 6 m wide; 4) ice fracture 12 m wide.

The fracture was covered by a polyethylene film 0.01 mm thick to eliminate the effect of water flooding on the bending of the rubber plate.

The experiments were performed in a  $5.0 \times 2.0 \times 0.5$  m tank equipped with a towing system. The model ice cover had dimensions of  $3.0 \times 1.4$  m. A diagram of the experimental setup is shown in Fig. 5. The model of the vessel is geometrically similar to the model used in the calculation. Towing of the model was performed under the model ice with a longitudinal open crack or an ice fracture of various widths ( $b_1 = 0.006$  m,  $b_2 = 0.012$  m,  $b_3 = 0.018$  m, and  $b_4 = 0.024$ ) at a relative submergence of the hull equal to 0.2. The obtained data were converted to nature according to the similarity conditions and a scale  $\lambda_l = 500$ . Figure 6 shows a curve of the maximum deflections of ice cover versus velocity SV. From Figs. 2 and 6, it follows that the data obtained in the experiments agree with the results of the calculations.

5. The results of the studies indicate that the mathematical model of ice bending taking into account inhomogeneities in the form of cracks and fractures is effective in the case of hydrodynamic loading of ice due to SV motion. Nevertheless, to take into account the interaction of the ice plate with waves on the free surface of the fracture, it is necessary to further refine the mathematical model by direct modeling of wave formation in the fracture. The error due to the approximate consideration of this interaction increases with increasing width of the fracture.

The results lead to the conclusion on the possibility of dynamic breaking of ice cover by a SV which performs translational motion under ice. The efficiency of breaking is increased if the SV moves along a longitudinal open crack at the resistant velocity.

## REFERENCES

1. V. M. Kozin, A. V. Onishchuk, E. N. Mar'uin, et al., *Ice-Breaking Capacity of Flexural-Gravity Waves Produced by Motion of Objects* [in Russian], Dal'nauka, Vladivostok (2005).
2. V. M. Kozin, *Resonant Method of Breaking Ice Cover: Inventions and Experiments* [in Russian], Akad. Estestvoznaniya, Moscow (2007).
3. V. M. Kozin and A. V. Onishchuk, "Model investigations of wave formation in solid ice cover from motion of a submarine," *J. Appl. Mech. Tech. Phys.*, **35**, No. 2. 235–238 (1994).
4. V. M. Kozin, V. D. Zhestkaya, A. V. Pogorelova, et al., *Applied Problems of Ice Cover Dynamics* [in Russian], Akad. Estestvoznaniya, Moscow (2008).
5. S. D. Chizhiumov, *Numerical Models in Problems of Ship Dynamics* [in Russian], Izd. Dal'nevost. Univ., Vladivostok (1999).
6. C. A. Brebbia, J. C. F. Telles, and L. C. Wrobel, *Boundary Element Techniques: Theory and Applications in Engineering*, Springer-Verlag, Berlin–New York (1984).
7. N. F. Ershov and A. N. Popov, *Strength of Ship Structures under Local Dynamic Loading* [in Russian], Sudostroenie, Leningrad (1989).
8. V. M. Kozin, "Modeling of flexural-gravity waves in a continuous ice cover," in: *Theory and Strength of an Ice-Breaking Ship* (collected scientific papers), No. 3, Gor'k. Politekh. Inst. (1982), pp. 35–38.